Revista ALCONPAT
www.revistaalconpat.org
eISSN 2007-6835
Revista de la Asociación Latinoamericana de Control de Calidad, Patología y Recuperación de la Construcción

Effect of the mix design method and concrete cover thickness of reinforced concrete on the relationship between resistivity and corrosion rate under natural marine exposure conditions.

J. A. Briceño-Mena[1,2], M. Soria-Castro[1,2], E. J. Pérez-García[3], D. Nieves-Mendoza[4], P. Castro-Borges[1]*
* Contact Author: pcastro@cinvestav.mx
DOI: https://doi.org/10.21041/ra.v16i3.1116

Received: 01/07/2026 | Received in revised form: 28/08/2026 | Accepted: 31/08/2026 | Published: 01/09/2026

ABSTRACT

This work aims to evaluate the effect of the design method and the concrete coating on the correlation between resistivity and corrosion rate. To this end, reinforced concrete specimens with volumetric design (M1) and aggregate packing (M2) were exposed to a tropical marine environment, and electrochemical parameters were measured periodically. The results showed equivalence between the two methods when the steel was kept in a passive state throughout the study period. However, during adjustments to the ρ-i_{corr} correlation, a discrepancy was found when increasing the coating: in M1, the adjustment deviated from the theoretical equations, whereas in M2, it approached them. When applying equations, attention should be paid to all conditions involving the element to avoid overestimating corrosion in the early stages.
Keywords: corrosion, electrical resistivity, corrosion rate, correlation, natural marine exposure.

Cite as: Briceño-Mena, J. A. Soria-Castro, M., Pérez-García, E. J., Nieves-Mendoza, D., Castro-Borges, P. (2026), *"Effect of the mix design method and concrete cover thickness of reinforced concrete on the relationship between resistivity and corrosion rate under natural marine exposure conditions."*, Revista ALCONPAT, 16 (3), pp. 521 – 535, DOI: https://doi.org/10.21041/ra.v16i3.1116

[1] Centro de Investigación y de Estudios Avanzados, Departamento de Física Aplicada, Km. 6 Antigua carretera a Progreso, Mérida, 97310, México.
[2] Secretaría de Ciencias, Humanidades, Tecnología e Innovación, Ciudad de México 03940, México.
[3] Ministerio de la Construcción de Cuba, La Habana 10699, Cuba.
[4] Facultad de Ingeniería Civil-Xalapa, Universidad Veracruzana, Xalapa, Veracruz 91000, México.

Contribution of each author
In this work, author Briceño-Mena contributed with experimentation (50%), development of a model (50%), data collection (100%), writing of the paper (50%) and discussion of results (30%); author Soria-Castro with experimentation (50%), discussion of results (20%); author Pérez-García with construction of test specimens (80%) and discussion of results (10%); author Nieves-Mendoza with construction of test specimens (20%) and discussion of results (10%); and author Castro-Borges with the original idea (100%), development of a model (50%) and writing of the paper (50%), in addition to discussion of results (30%)

Discussions and subsequent corrections to the publication
Any dispute, including the replies of the authors, will be published in the second issue of 2027 provided that the information is received before the closing of the first issue of 2027.

Efecto del método de dosificación y del espesor de recubrimiento del concreto reforzado sobre la relación entre la resistividad y la velocidad de corrosión en condiciones de exposición marina natural

RESUMEN

Este trabajo tiene como objetivo evaluar el efecto del método de diseño y del recubrimiento de concreto sobre la correlación entre la resistividad y la velocidad de corrosión. Para ello, se expusieron probetas de concreto reforzado con un diseño volumétrico (M1) y un empaquetamiento de agregados (M2) en un ambiente marino tropical, y se midieron periódicamente los parámetros electroquímicos. Los resultados mostraron equivalencia entre ambos métodos al mantener el acero en estado pasivo durante el período estudiado. Sin embargo, en los ajustes de la correlación ρ-i_{corr} se encontró una disparidad: al aumentar el recubrimiento, en M1 el ajuste se alejaba de las ecuaciones teóricas y en M2 se acercaba. Al aplicar ecuaciones, se debe prestar atención a todas las condiciones que involucren al elemento para no sobreestimar la corrosión en etapas iniciales.

Palabras clave: corrosión, resistividad eléctrica, velocidad de corrosión, correlación, exposición marina natural

Efeito do método de dosagem e da espessura da camada de concreto armado na relação entre a resistividade e a taxa de corrosão sob condições naturais de exposição marinha.

RESUMO

Este estudo teve como objetivo avaliar o efeito do método de dimensionamento do concreto e da espessura do cobrimento sobre a correlação entre a resistividade e a taxa de corrosão. Para tanto, corpos de prova de concreto armado com dimensionamento volumétrico (M1) e dimensionamento por compactação de agregados (M2) foram expostos a um ambiente marinho tropical, e os parâmetros eletroquímicos foram medidos periodicamente. Os resultados mostraram equivalência entre os dois métodos quando o aço foi mantido em estado passivo durante o período de estudo. Contudo, observou-se uma discrepância no ajuste da correlação ρ-i_{corr}: com o aumento da espessura do cobrimento, o ajuste se desviou das equações teóricas em M1 e se aproximou delas em M2. Ao aplicar as equações, deve-se atentar a todas as condições que envolvem o elemento, a fim de evitar a superestimação da corrosão nos estágios iniciais.

Palavras-chave: corrosão, resistividade elétrica, taxa de corrosão, correlação, exposição marinha natural

Legal Information

Revista ALCONPAT is a quarterly publication by the Asociación Latinoamericana de Control de Calidad, Patología y Recuperación de la Construcción, Internacional, A.C., Km. 6 antigua carretera a Progreso, Mérida, Yucatán, 97310, Tel. +52 1 983 419 8241, alconpat.int@gmail.com, Website: www.alconpat.org

Reservation of rights for exclusive use No.04-2013-011717330300-203, and ISSN 2007-6835, both granted by the Instituto Nacional de Derecho de Autor. Responsible editor: Pedro Castro Borges, Ph.D. Responsible for the last update of this issue, Informatics Unit ALCONPAT, Elizabeth Sabido Maldonado.

The views of the authors do not necessarily reflect the position of the editor.

1. INTRODUCTION

The corrosion of reinforcing steel in concrete, induced by aggressive agents such as chlorides, is the most common form of deterioration in infrastructure of tropical marine environments (Qu et al., 2021). The evidence in the literature on the aggressive environment along the Yucatecan coast in the Gulf of Mexico suggests that this region is a natural laboratory for extreme atmospheric corrosivity (Maldonado & Veleva, 1999). In this scenario, the durability of reinforced concrete is key and is determined by the resistance to ion flow through the cementitious microstructure (Abraham & Mathew, 2021; Azarsa & Gupta, 2017). Because of this, controlling variables such as the water/cement ratio (w/c), resistivity, and coating thickness is key to prolonging the useful life and maintaining optimal performance of the structures (Balestra et al., 2019; Castañeda Valdés et al., 2024). Under these circumstances, the use of durability parameters is increasingly common in national and international regulations, such as NMX-C-530 (2017) in Mexico. This standard highlights electrical resistivity as a fundamental performance criterion that reflects the interaction between the material's intrinsic characteristics and environmental variations.

Historically, resistivity has served as a bridge to evaluate electrochemical kinetics. Several authors have formalized mathematical relationships based on resistivity, as is the case with Andrade (1988), who proposes estimating the corrosion rate through the relationship $i_{corr} = 26\ \rho^{-1}$, which, in its mathematical form, follows the structure $y = A\ \rho^{B}$. However, evidence indicates that this inverse correlation (known as the R-C relationship) is not universal (Torres-Acosta, 2024). The influence of humidity, temperature, ion concentration, and material properties nonlinearly modifies resistive electrical properties and activity at the steel-concrete interface (Zhang et al., 2021). Additionally, chemical factors, such as the nature of the cementitious material and the pH of the pore solution, can affect the correlation. For example, a decrease in pH increases the material's resistivity during carbonation and, at the same time, accelerates corrosion by decreasing the $[Cl^-]/[OH^-]$ ratio, thereby completely modifying the theoretical curves (Tian & Ye, 2022). In addition, under active corrosion conditions, corrosion rates exhibit greater fluctuations than those observed in resistivity measurements, increasing the margin of uncertainty in theoretical estimates (Pedrosa & Andrade, 2021; Rodrigues et al., 2021).

The above shows the need to use calibrated models under similar exposure conditions, whether in real, laboratory, prolonged, or short-range exposures. In addition, they could lack precision if the influence of geometric design, dosages, or spatial position are ignored (Briceño-Mena et al., 2019) (Koleva et al., 2008). In the first instance, the coating thickness acts as a physical barrier that can delay the onset of corrosion, and the w/c ratio can determine the network of interconnected pores through which aggressive agents are transported. The correlation between electrical resistivity and corrosion rate does not depend solely on a single property but on a set of factors that can modify them simultaneously or in opposite directions. The authors listed in Table 1 present factors that affect the resistivity and corrosion of steel, as these precisely account for the dispersion observed in the theoretical equations. Some of these parameters shift resistivity and corrosion in the same direction, while others do so in the opposite direction. For example, the degree of saturation mentioned by Kim (2026) and Zhang (2021) and the w/c ratio mentioned by Azarsa and Gupta (2017) influence in opposite directions: increasing them reduces resistivity and increases the risk of corrosion. Carbonation, on the other hand, acts simultaneously: it raises resistivity and increases the risk of corrosion, as mentioned by Azarsa and Gupta (2017).

Table 1. Material and environmental parameters influencing the correlation between corrosion and resistivity in concrete.

Author	**Parameter**	**Effect on resistivity**	**Effect on corrosion**
(Kim et al., 2026) (Zhang et al., 2021)	Degree of saturation	It decreases exponentially with increasing saturation (R^2 between 0.896 and 0.997).	Increases the risk of corrosion. Promotes chloride migration
(Morris et al., 2004) (Liu et al., 2024)	Chloride concentration	When the electrical resistivity of concrete increases between 2 and 100 kΩ·cm, the threshold value goes from 0.44% to 2.32%	Decreases the anodic slope of Tafel by increasing the concentration at any value (above 0%)
(Morris et al., 2004) (Le et al., 2021)	Temperature	It affects pore saturation and therefore resistivity. As the temperature increases, the resistivity decreases	Influences electrochemical kinetics
(Azarsa & Gupta, 2017)	Water/cement ratio	Higher w/c ratio, lower resistivity due to higher porosity	Increased susceptibility to corrosion
(Azarsa & Gupta, 2017)	Carbonation	Forms a multi-layer resistivity profile	Changes corrosion mechanisms

Table 2 presents the empirical correlations reported in the literature, elaborated from information provided by Torres-Acosta (2024). The table was ordered in descending order based on the correlation coefficients (R^2), indicators of the equation's reliability. Unlike the exponent, trend indicator, and coefficient (multiplier), which indicate magnitude, R^2 is relevant for deciding which equation to use. The table shows that in a marine environment, R^2 falls to 0.43. This could be attributed in part to the internal conditions of humidity and temperature, in combination with the movement of chlorides, a product of different penetration mechanisms, which influence the degree of saturation of the pores and even the development of porosity, a product of the continuous hardening of the concrete. On the other hand, in CO_2-containing environments, the estimate achieves a high level of reliability, close to 1 (R^2 = 0.93). This could be attributed to carbonation considerably reducing the effective porosity and increasing the density of the concrete, thereby favoring a more stable resistivity over time. On the other hand, as a new generalized theoretical approach, Torres-Acosta (2024) proposes using the equation obtained by integrating the various studies discussed in Table 2.

Table 2. Correlation equations between resistivity and corrosion rate from various authors.

Author	Exposure Condition	Specimens	Cementing agent	w/c ratio	Measurement method, i_{corr}	Measurement method, ρ	Fitting equation	R^2
(Hornbostel et al., 2017)	Saline immersion	Reinforced mortar prisms	With fly ash substitutions	0.4 and 0.55	Galvanic Current	LCR (Inductance, Capacitance, and Resistance) Meter	$i_{corr}=208.27\rho^{\wedge -0.603}$	0.4263
(Rodriguez et al., 1993)	Natural marine	Real Reinforced Concrete Structures	-	-	Resistance to linear polarization	In-house equipment with guard ring and sensors	$i_{corr}=2.8785\rho^{\wedge -0.766}$	0.5027
(Andrade, 2018)	Chlorides	High-quality concrete	-	-	-	Direct method/Wenner method	$i_{corr}=207.68\rho^{\wedge -1.335}$	0.6188
(Presuel -Moreno et al., 2018) .	Moisture-drying cycles in natural saline/marine solution	Reinforced concrete prisms	With fly ash substitutions, silica fume	Miscellaneous	Resistance to polarization	Direct	$i_{corr}=7.6144\rho^{\wedge -1.058}$	0.822
(Torres-Acosta et al., 2005) .	Moisture-drying cycles in saline solution	Reinforced concrete prisms	With nopal and aloe substitutions	-	Resistance to linear polarization	-	$i_{corr}=24.965\rho^{\wedge -1.439}$	0.8484
Geiker et al.	Accelerated carbonation	Concrete prisms	-	-	Commercial Corrosimeter	Commercial Corrosimeter	$i_{corr}=26.378\rho^{\wedge -0.959}$	0.9225
(Torres-Acosta & González-Calderón, 2021)	Natural carbonation	Mortars	-	-	Resistance to polarization	Electrical resistance	$i_{corr}=16.452\rho^{\wedge -0.919}$	0.9395
(Torres-Acosta, 2024)	All of the above conditions						$i_{corr}=7.1\rho^{\wedge -0.81}$	0.7813

The dependence and convenience of using resistivity values to infer corrosion rates has grown, so that in many types of research the same type of equation has been proposed, discussed above, but with different correlation coefficients associated with reinforced concrete properties and exposure conditions that cannot be easily discriminated when comparing different types of study. As a consequence, it is not yet possible to speak about a law that allows correlating resistivity with corrosion rate at 100%, at least until more data are available.
Currently, most available studies have been conducted under controlled laboratory conditions, which tend to oversimplify the degradation mechanisms that occur in natural environments. Hence, there is a need to generate empirical data to enrich existing models.
Therefore, the present work aims to present and discuss the results for resistivity and corrosion rate derived from the exposure of reinforced concrete specimens from the DUCONDOS project (Durability comparison with two design methods) in a tropical marine environment in Telchac Puerto, Yucatán, over approximately 1300 days. The analysis focuses exclusively on the correlation between resistivity and corrosion rate, derived from interactions among the water/cement ratio, coating thicknesses, and the use of two mix design methods.

2. METHODOLOGY

The methodological design aimed to verify correlations among the mix design parameters, coating thicknesses, and the electrochemical behavior of the reinforcing steel, depending on the design method used.

2.1 Manufacture of specimens.

The experimental methodology contemplated the manufacture of 12 specimens of reinforced concrete, designed with two different methods, six for each method (two w/c ratios):

- Method 1 (M1), based on the ultimate resistance of the elements and the absolute volume of the materials, contemplates the conventional procedure used in our region and worldwide (ACI Committee 211, 2022).
- Method 2 (M2), which considers particle size distribution and an adequate arrangement of the aggregates. Its main characteristic is to minimize voids in the concrete matrix (O'Reilly, 1990).

Table 3 presents the dosages per unit volume (m³) of the M1 and M2 designs. Among the similarities, both designs consider aggregate absorption and moisture. Among the differences, the amount of aggregates in M2 was evidently higher, especially in fine aggregate, to achieve efficient packing between coarse particles and to fill the gaps. As a direct consequence of the granular arrangement, the cement consumption required for the mixture was slightly lower in M2 than in M1.

Table 3. Material dosage according to each mix design method.

Material	Method 1		Method 2	
	w/c ratio 0.45	w/c ratio 0.65	w/c ratio 0.45	w/c ratio 0.65
Cement	408	277	404	274
Powder	681	739	728	790
Gravel	800	868	758	823
Water	187	180	185	177

[1] The quantities given are in kg/m³, and the aggregates were corrected for their moisture content.

The mixtures were made with CPC-30R cement, common in the exposure area, and crushed limestone aggregates were used, extracted from material banks in the region. As observed in Table

3, two w/c ratios, 0.45 and 0.65, were used, which resemble the ideal conditions and those commonly used in small works. Therefore, 3 specimens were constructed for each method and each w/c ratio. The manufactured specimens have a cross-section of 150 x 150 mm and a length of 300 mm. Six carbon steel bars of 9.5 mm (3/8") in diameter and 500 mm in length were used, with coatings of 15 mm, 20 mm, and 30 mm thick, and 3 access chambers were placed at the height of the rebar, as shown in Figure 1. In this work, only the results for a w/c ratio of 0.45 in both design methods are analyzed.

Figure 1. Specimen and its exposure scheme; the major coating is in the lower bed.

2.2 Environmental exposure.
The study was carried out at the Cinvestav Mérida marine station in Telchac Puerto, Yucatán, under an environmental exposure classified as CX (atmospheric corrosion). The exposure site is located 50 m from the coastline and 0.95 m above ground level. The specimens were oriented so that the faces to be studied were exposed to the prevailing northeasterly winds, leaving the bar with the greatest coating (30 mm) at the bottom, following the scheme of natural exposure stations used in previous studies of durability in tropical marine environments (Figure 2). (ISO 9223:2012, 2012) (Castañeda Valdés et al., 2024; Troconis De Rincón et al., 2015).

Figure 2. Specimen exposure area.

2.3 Electrochemical, electrical and environmental parameters.
For approximately 1300 days, electrochemical and electrical monitoring was conducted to assess the behavior of the specimens. However, these measurements did not follow a fixed sequence relative to one another due to the natural exposure conditions. The monitoring was carried out using a commercial corrosimeter (Gcorr 6), equipped with a sensor with signal confinement placed at the center of the specimens and a connection cable to the working electrode. This arrangement allows measurement of the corrosion potential (E_{corr}) in mV, the corrosion velocity (i_{corr}) in µA/cm², and the electrical resistance of the concrete, which helps to determine its resistivity (ρ) in kΩ·cm.
The internal recording of the environmental conditions of the specimens was obtained by means of a temperature and humidity probe that was introduced into the interior of the concrete

3. RESULTS

This section presents results only for corrosion rates and point resistivities over time, showing periodicities driven by environmental conditions.

3.1 Corrosion rate.

Figure 3 shows the corrosion rates obtained over approximately 1300 days for the three coating thicknesses of specimens M1 and M2 with a w/c ratio of 0.45. The effect of the w/c ratio on electrochemical kinetics is clearly observed; i_{corr} results below the depassivation threshold (0.1 µA/cm²) are consistently observed. The minor fluctuations respond directly to the natural wetting and drying cycles of the coastal climate and are attributable to the dense matrix, regardless of coating thickness (15, 20, or 30 mm).

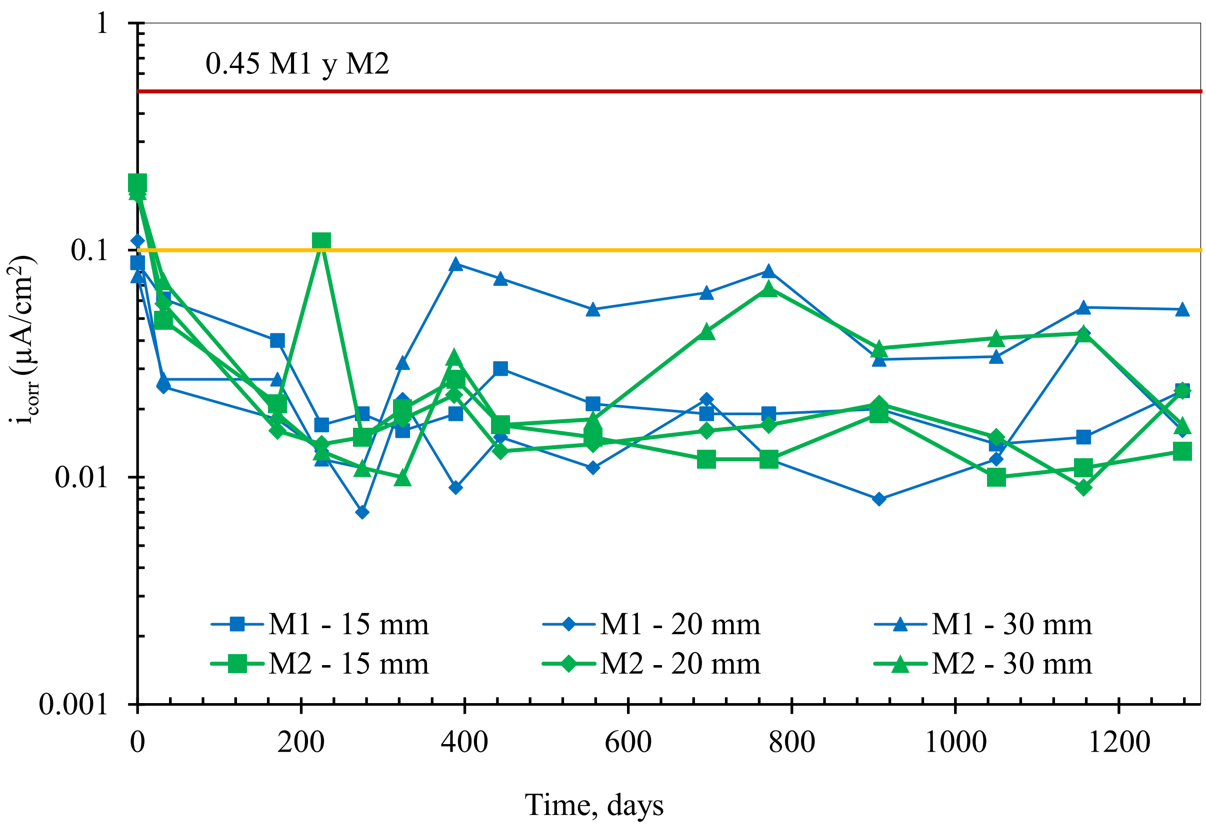

Figure 3. Corrosion rate of specimens in methods M1 and M2.

3.2 Resistivity

Figure 4 presents the specific results of the electrical resistivity over time for the three coating thicknesses of the M1 and M2 specimens. In these, two stages can be observed: the first, when the concrete is in the first phases of hydration and presents resistivities of around 10 kΩ·cm; and, after one year, the values tend to increase considerably, consistent with the hydration process and, consequently, with the refinement of the pore network.

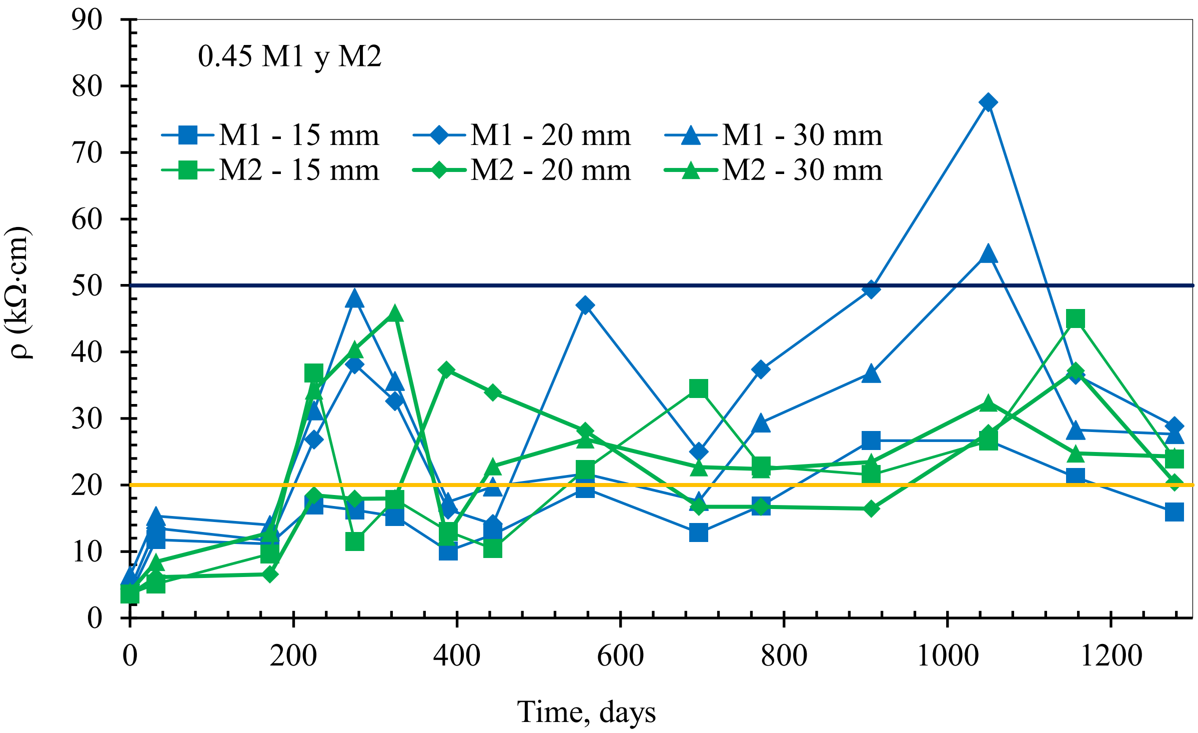

Figure 4. Electrical resistivity of specimens in the M1 and M2 methods.

4. DISCUSSION

The results showed that over 1300 days of natural exposure, a low w/c ratio in both mix design methods yields concrete with equivalent electrochemical behavior. This shows that, although the method is based on particle-size redistribution that, above all, raises the fines content, it allows a passive state even under such aggressive site conditions. Therefore, granular readjustment does not compromise the durability of good-quality concretes or aspects such as strength, cost, carbon footprint, and microstructure, as demonstrated by Murillo Mosquera et al. (2025)

To conduct a more in-depth analysis of the results, Figures 5 and 6 show the correlations between resistivity and corrosion rates for M1 and M2, respectively. Figure 5 presents the analysis of M1, where a degradation of the fit is observed as the depth of the steel increases: in the most superficial coating, a R^2 of 0.75 is observed; as the coating depth increases, the R^2 decreases to 0.20. The comparative performance of method 2 (M2) presented in Figure 6 is of interest. Despite operating with a different design from the traditional volumetric (M1), the optimization of aggregate arrangement implemented in M2 maintained resistivity and corrosion rate values that were statistically comparable to or superior to those of M1. This shows that minimizing voids through particle-size selection does not compromise durability against chloride penetration.

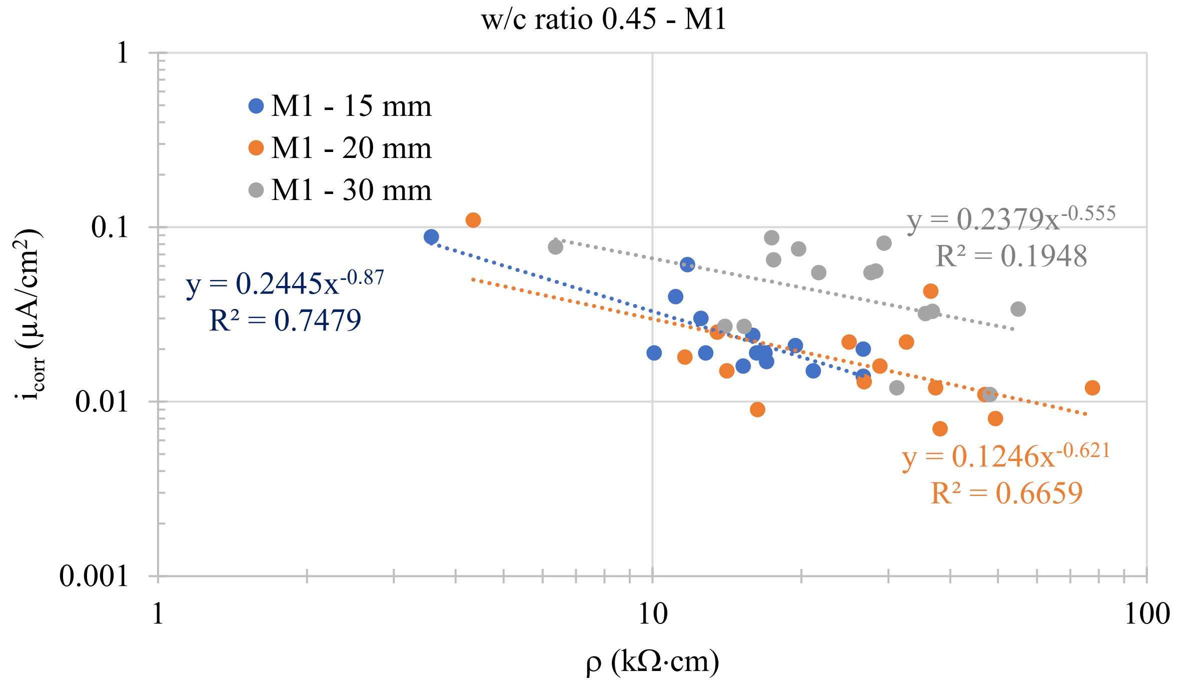

Figure 5. Correlation between electrical resistivity and corrosion rate of M1 as a function of coating thickness.

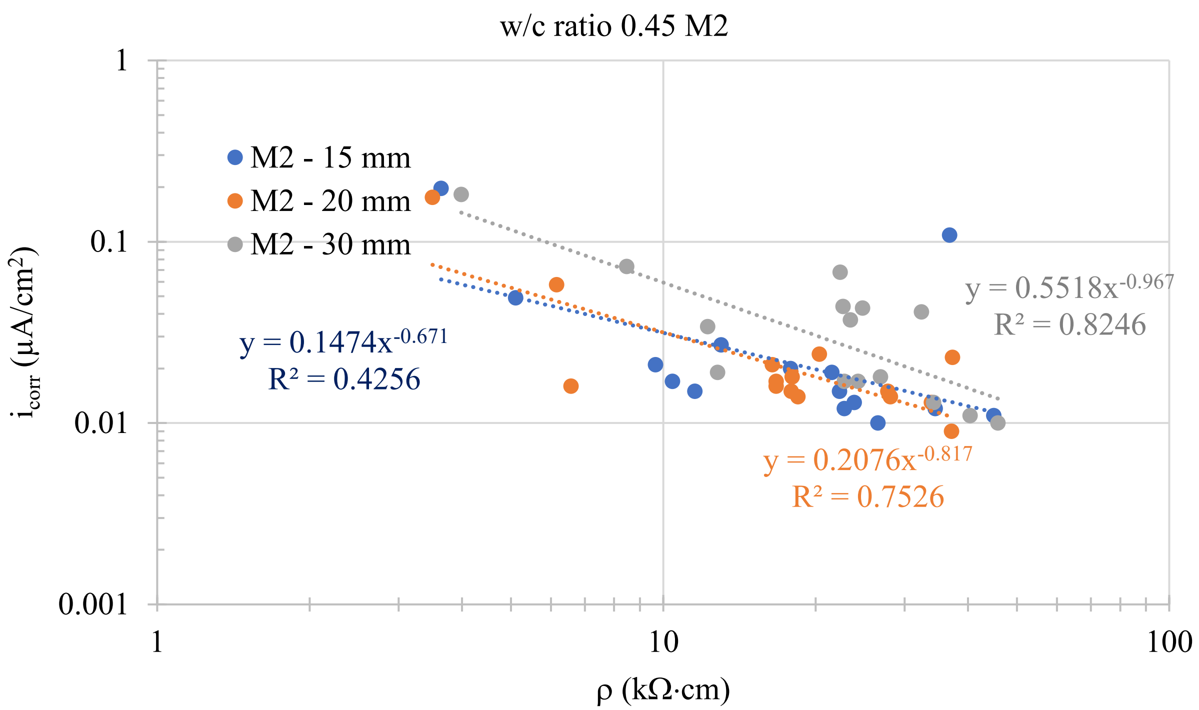

Figure 6. Correlation between electrical resistivity and corrosion rate of M2 as a function of coating thickness.

By projecting the overall correlation between resistivity and corrosion rate from all experimental data obtained in each test method (M1 and M2), without distinguishing between coating thicknesses (15 mm, 20 mm, and 30 mm), the dispersion of natural monitoring takes center stage. The data cloud, constantly shaped by the temperature and humidity gradients within the specimens,

generates a model that deviates from the proportionality implied by the -1 exponent in Andrade's theoretical equation. The changing conditions of real exposure make the empirical slope more moderate, meaning that, in outdoor marine structures under conditions similar to those in this study, resistivity loses part of its predictive capacity, regardless of coating thickness, at least in the Tuutti initiation stage. This becomes important due to interactions, even when the steel is passivated, with other factors that influence the reinforced concrete (w/c ratio, degree of saturation, temperature, chloride content, carbonation, among others). This entails the careful use of equations and predictive models of corrosion kinetics, as well as complementary techniques to confirm them.
Especially when it comes to large infrastructure works, where engineers must employ wider safety margins when assessing the kinetics of damage (1982)
A general analysis of the points could give an idea of what happens if criteria such as the element's geometry or its conditions are not considered. Figure 7 presents the general correlations of M1. By projecting all the data on a single graph, without differentiating the coating thicknesses, the dispersion generated by natural monitoring in the initial stages is observed. The data cloud groups the microclimates generated at each depth, resulting in a line that averages heterogeneous behaviors and deviates from the theoretical model.

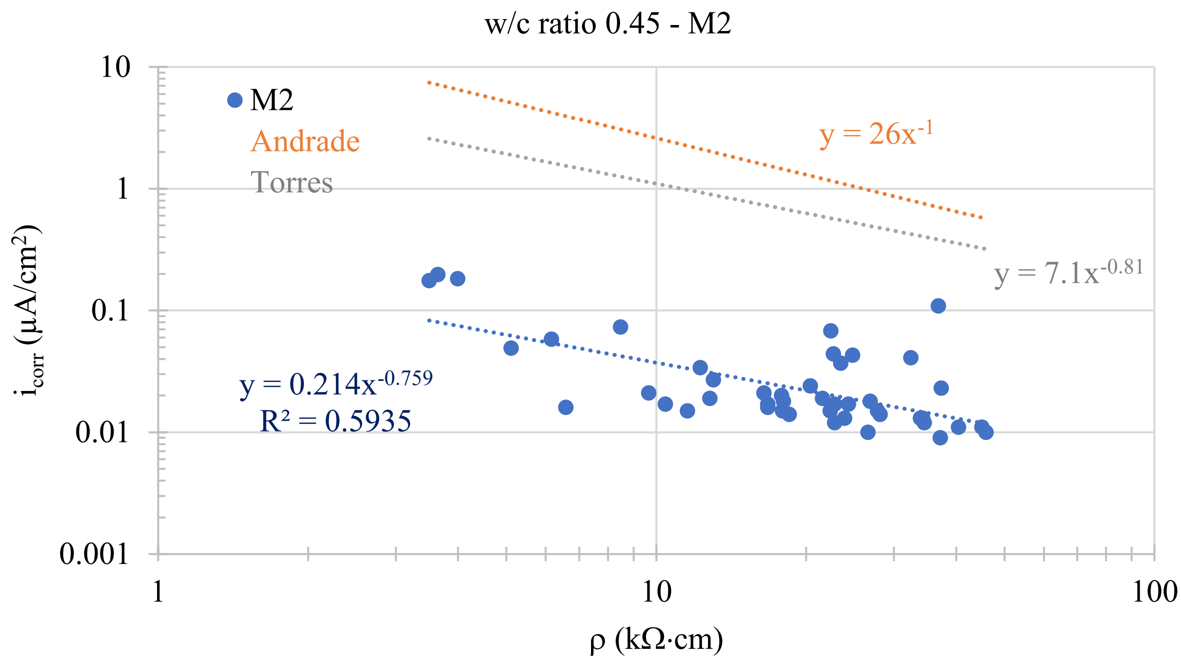

Figure 7. General correlation between electrical resistivity and corrosion rate of M1.

The comparative performance of M2, as shown in Figure 8, is notable for better equation coupling, a higher R^2, and a slope closer to 1. However, the data cloud also reflects variability in weathering and demonstrates that minimizing voids through granular selection is an effective design method for low w/c ratios.

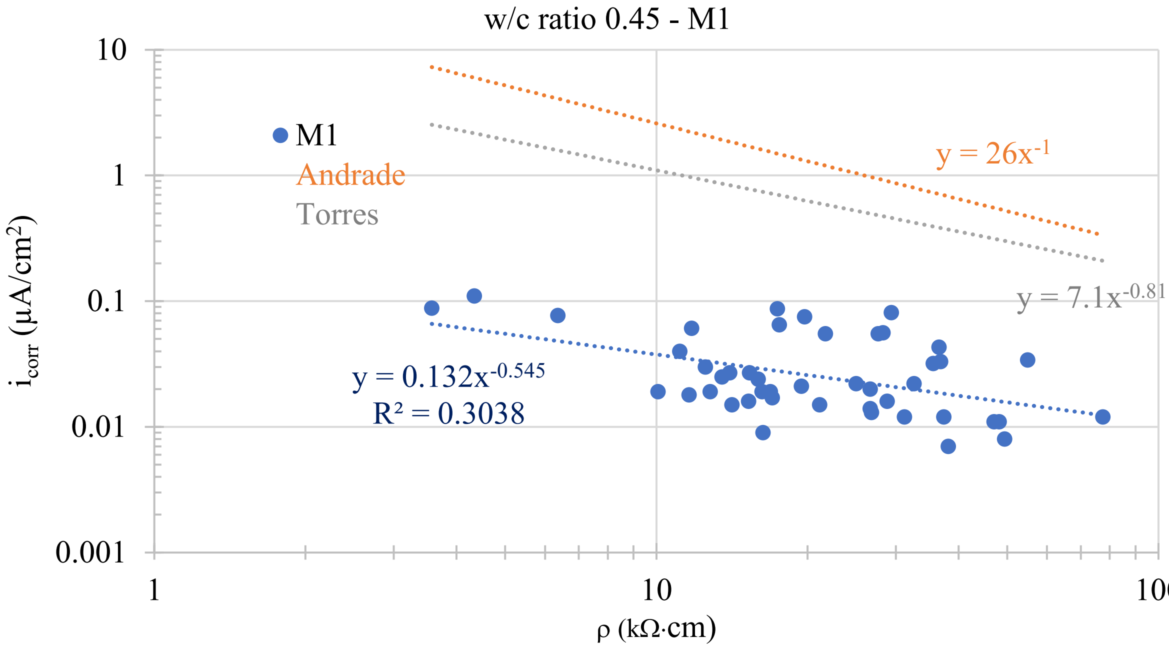

Figure 8. General correlation of electrical resistivity and corrosion rate of M2.

The presentation of correlations by coating thickness was established to observe what happens when three depths with different levels of electrochemical activity are not grouped together, since a correlation could be generated between the different coatings. Presenting the individual values by depth, with their trend line and equation, allows us to assess whether the overall fit reflects homogeneous behavior or incorporates disparate behavior. As can be seen in Table 5, the latter occurs, since the exponents per coating vary between -0.555 and -0.87, with a general value of -0.545, for M1, and between -0.671 and -0.967, with a general value of -0.759, for M2. The general adjustment should not be understood as a property of the material, but as the sum of the contributions of the internal microclimates in each coating depth.

Table 5. Summary of the single and general correlations of M1 and M2.

Method	Coating(mm)	Equation	R^2
M1	15	$y = 0.2445\ \rho^{-0.87}$	0.75
M1	20	$y = 0.1246\ \rho^{-0.621}$	0.67
M1	30	$y = 0.2379\ \rho^{-0.555}$	0.20
	General	$y = 0.132\ \rho^{-0.545}$	0.30
M2	15	$y = 0.1474\ \rho^{-0.671}$	0.43
M2	20	$y = 0.2076\ \rho^{-0.817}$	0.75
M2	30	$y = 0.5518\ \rho^{-0.967}$	0.83
	General	$y = 0.214\ \rho^{-0.759}$	0.59

As shown in Table 5, the adjustments as a function of coating thickness differ between the two methods in opposite directions. That is, in M1, the coefficient R^2 and the exponents move away from unity as the coating increases, while in M2 they approach unity as the coating increases. In other words, the correlation between resistivity and corrosion rate for M2, based on aggregate arrangement, fits better with the equations described in the literature as the coating thickness increases, whereas M1, based on absolute volumes, degrades. This could be explained by the internal microclimate, which remains stable thanks to the arrangement of the aggregates. However, it must be corroborated by physical tests and not attributed solely to the coating.

5. CONCLUSIONS

From the electrochemical evaluation of concrete specimens designed by two methods and in relation to w/c, exposed to a tropical marine environment for approximately 1300 days, the following conclusions are established:

- Low w/c ratio control allows reinforcing steel to be kept passive in the face of marine conditions regardless of coating thickness or design method.
- The M2 proved to be a viable design alternative. The arrangement of the aggregates allowed a resistive evolution consistent with M1.
- The correlation between resistivity and corrosion rate is influenced by the geometry of the specimen and by the mix design method of the concrete. The estimation equations were misaligned and exhibited inconsistent behavior, likely due to environmental influences.
- The design of the mixture affects the stability of the internal microclimate in the face of environmental changes.
- In the M1 method, the self-model obtained degraded as the coating thickness increased. In the M2 method, the mathematical approximation is best fitted when entering the concrete.

6. ACKNOWLEDGEMENTS

The authors thank Eng. Mercedes Balancán Zapata and M.C. Alexia Zozaya for their support in obtaining results and analyzing data. Special posthumous thanks to Dr. Vitervo O'Reilly, who was the creator of the M2 method.

7. REFERENCIAS

Abraham, B., Mathew, J. (2021). *A Review on Durability Assessment of Concrete Structures Using Electrical Resistivity Method.* International Journal of Research in Engineering and Science (IJRES) ISSN, 9(7), 12–19. www.ijres.org

ACI Committee 211. (2022). *Selecting Proportions for Normal-Density and High-Density Concrete-Guide.* American Concrete Institute. www.concrete.org

Alonso, C., Andrade, C., González, J. A. (1988). *Relation between resistivity and corrosion rate of reinforcements in carbonated mortar made with several cement types.* Cement and Concrete Research, 18(5), 687–698. https://doi.org/10.1016/0008-8846(88)90091-9

Andrade, C. (2018). *Diseño y evaluación de la vida útil a través de resistividad eléctrica concreta.* Revista ALCONPAT, 8(3), 264–279. https://doi.org/10.21041/ra.v8i3.349

Azarsa, P., Gupta, R. (2017). *Electrical Resistivity of Concrete for Durability Evaluation: A Review.* Advances in Materials Science and Engineering, 2017. https://doi.org/10.1155/2017/8453095

Balestra, C. E. T., Nakano, A. Y., Savaris, G., Medeiros-Junior, R. A. (2019). *Reinforcement corrosion risk of marine concrete structures evaluated through electrical resistivity: Proposal of parameters based on field structures.* Ocean Engineering, 187. https://doi.org/10.1016/j.oceaneng.2019.106167

Briceño-Mena, J. A., Balancán-Zapata, M. G., Castro-Borges, P. (2019, November 30). *EFECTO BORDE EN EL PROCESO DE CORROSIÓN A EDADES TEMPRANAS.* MEMORIAS CONPAT 2019. https://doi.org/10.21041/CONPAT2019/V1CC388

Castañeda Valdés, A., Corvo Pérez, F., Pech Pech, I., Marrero Águila, R., Bastidas-Arteaga, E.

(2024). *Durability Requirements for Reinforced Concrete Structures Placed in a Hostile Tropical Coastal Environment.* Buildings, 14(8). https://doi.org/10.3390/buildings14082494

Geiker, M. Hornsbostel, K. Belda Revert, A. (2019), "*Corrosion Rate; Experimental Observations in Carbonated or Chloride Containing Concrete.*" in Proceedings of the Mathematical Models of Reinforcement Corrosion and its Consequences for Structural Performance, Paris, France, Oct. 28–29.

Hornbostel, K., Elsener, B., Angst, U. M., Larsen, C. K., Geiker, M. R. (2017). *Limitations of the use of concrete bulk resistivity as an indicator for the rate of chloride-induced macro-cell corrosion.* Structural Concrete, 18(2), 326–333. https://doi.org/10.1002/suco.201500141

Industria de La Construcción – Durabilidad – Norma General de Durabilidad de Estructuras de Concreto Reforzado – Criterios y Especificaciones, 1 (2017).

ISO 9223:2012. (2012). *Corrosion of metals and alloys — Corrosivity of atmospheres — Classification, determination and estimation*. EUROPEAN STANDARD.

Kim, Y., Kee, S. H., Monjardin, C. E. F., Robles, K. P. V. (2026). *Multivariate Machine Learning Framework for Predicting Electrical Resistivity of Concrete Using Degree of Saturation and Pore-Structure Parameters.* Materials, 19(2). https://doi.org/10.3390/ma19020349

Koleva, D. A., de Wit, J. H. W., van Breugel, K., Veleva, L. P., van Westing, E., Copuroglu, O., Fraaij, A. L. A. (2008). *Correlation of microstructure, electrical properties and electrochemical phenomena in reinforced mortar. Breakdown to multi-phase interface structures. Part II: Pore network, electrical properties and electrochemical response*. Materials Characterization, 59(6), 801–815. https://doi.org/10.1016/j.matchar.2007.06.016

Le, H. V., Kim, M. K., Kim, D. J., Park, J. (2021). *Electrical properties of smart ultra-high performance concrete under various temperatures, humidities, and age of concrete.* Cement and Concrete Composites, 118. https://doi.org/10.1016/j.cemconcomp.2021.103979

Liu, Q., Pei, G., Chen, L., Duan, K., Zhang, F., Su, R. K.-L. (2024). *Effects of Chloride, Humidity, and Concrete Mix on the Electrochemical Parameters of Steel Reinforcement Corrosion.* Journal of Materials in Civil Engineering, 36(8). https://doi.org/10.1061/jmcee7.mteng-17914

Maldonado, L., Veleva, L. (1999). *Corrosivity category maps of a humid tropical atmosphere: the Yucatán Peninsula, México.* Materials and Corrosion, 50, 261–266.

Morris, W., Vico, A., Vázquez, M. (2004). *Chloride induced corrosion of reinforcing steel evaluated by concrete resistivity measurements.* Electrochimica Acta, 49(25), 4447–4453. https://doi.org/10.1016/j.electacta.2004.05.001

Murillo Mosquera, E., Cifuentes, S., Obando, J. C., Monteiro, S. N., Colorado, H. A. (2025). *Concrete Obtained with the Viterbo O'Reilly Method for Aggregate Gradation: A Potential Model for Sustainable Design and Reducing Development Costs.* Materials, 18(15). https://doi.org/10.3390/ma18153558

O'Reilly, V. A. (1990). *Métodos para Dosificar Mezclas de Hormigón* (1a edición). Científico-Técnico.

Pedrosa, F., Andrade, C. (2021). *Spatial variability of concrete electrical resistivity and corrosion rate in laboratory conditions.* Construction and Building Materials, 306. https://doi.org/10.1016/j.conbuildmat.2021.124777

Presuel-Moreno, F., Bencosme, R., Hoque, K., Nazim, Manzurul, Kazemi, A., Tang, F. (2018). *Corrosion Propagation of Carbon Steel Rebars in High Performance Concrete*.

Qu, F., Li, W., Dong, W., Tam, V. W. Y., Yu, T. (2021). *Durability deterioration of concrete under marine environment from material to structure: A critical review.* Journal of Building Engineering, 35. https://doi.org/10.1016/j.jobe.2020.102074

Rodrigues, R., Gaboreau, S., Gance, J., Ignatiadis, I., Betelu, S. (2021). *Reinforced concrete structures: A review of corrosion mechanisms and advances in electrical methods for corrosion monitoring.* In Construction and Building Materials (Vol. 269). Elsevier Ltd.

https://doi.org/10.1016/j.conbuildmat.2020.121240
Rodriguez, J., Ortega, L., García, A. (1993, December). *On Site Corrosion Rate Measurements in Concrete Structures.* Hormigón y Acero.
Tian, Z., Ye, H. (2022). *Mechanisms underlying the relationship between electrical resistivity and corrosion rate of steel in mortars.* Cement and Concrete Research, 159. https://doi.org/10.1016/j.cemconres.2022.106867
Torres-Acosta, A. A. (2024). *Technical Note: Considerations to Avoid Corrosion Rate Estimate Error of the Reinforcing Steel if Based Only on Concrete's Electrical Resistivity*. Corrosion, 80(4), 332–337. https://doi.org/10.5006/4482
Torres-Acosta, A. A., González-Calderón, P. Y. (2021). Opuntia ficus-indica (OFI) mucilage as corrosion inhibitor of steel in CO2-contaminated mortar. Materials, 14(5). https://doi.org/10.3390/ma14051316
Torres-Acosta, A. A., Martínez-Madrid, M., Loveday, D., Horner, M. (2005, March 3). *Nopal and Aloe Vera Additions in Concrete Electrochemical Behavior of the Reinforcing Steel*. CORROSION 2005.
Troconis De Rincón, O., Montenegro, J. C., Vera, R., Carvajal, A. M., Mejía De Gutierrez, R., Del Vasto, S., Saborio, E., Torres-Acosta, A., Pérez-Quiroz, J., Martínez-Madrid, M., Martinez-Molina, W., Alonso-Guzmán, E., Castro- Borges, P., Moreno, E. I., Almeraya-Calderón, F., Gaona-Tiburcio, C., Pérez-López, T., Salta, M., De Melo, A. P., … De Partidas, E. (2015). *Concrete carbonation in Ibero-American countries DURACON project: Six-year evaluation.* Corrosion, 71(4), 546–555. https://doi.org/10.5006/1385
Tuutti, K. (1982). *Corrosion of steel in concrete.* Swedish Cement and Concrete Research Institute, 473.
Zhang, G., Zhu, Y., Lin, X., Tian, Y., Ye, H., Jin, X., Jin, N., Yan, D., Xiao, F., Yao, K., Chen, J. (2021). *Numerical simulation of electrochemical mechanism of steel rebar corrosion in concrete under natural climate with time-varying temperature and humidity.* Construction and Building Materials, 306. https://doi.org/10.1016/j.conbuildmat.2021.124873